

# RaLP, a New Member of the Src Homology and Collagen Family, Regulates Cell Migration and Tumor Growth of Metastatic Melanomas

Ernesta Fagiani,<sup>1</sup> Giuseppina Giardina,<sup>1</sup> Lucilla Luzi,<sup>1,2</sup> Matteo Cesaroni,<sup>1,2</sup> Micaela Quarto,<sup>1,2</sup> Maria Capra,<sup>1,2</sup> Giovanni Germano,<sup>1</sup> Maria Bono,<sup>4</sup> Manuela Capillo,<sup>1</sup> PierGiuseppe Pelicci,<sup>1,2,3</sup> and Luisa Lanfrancone<sup>1</sup>

<sup>1</sup>Department of Experimental Oncology, European Institute of Oncology; <sup>2</sup>Institute of Molecular Oncology of the Italian Foundation for Cancer Research; <sup>3</sup>Dipartimento di Medicina, Chirurgia ed Odontoiatria, Università degli Studi di Milano, Milan, Italy; and <sup>4</sup>IFOM Centre of Cell Oncology and Ultrastructure, Department of Experimental Medicine, Genova, Italy

## Abstract

The Src homology and collagen (Src) family of adaptor proteins comprises six Shc-like proteins encoded by three loci in mammals (Shc, Rai, and Sli). Shc-like proteins are tyrosine kinase substrates, which regulate diverse signaling pathways and cellular functions, including Ras and proliferation (p52/p46Shc), phosphatidylinositol 3-kinase and survival (p54Rai), and mitochondrial permeability transition and apoptosis (p66Shc). Here, we report the identification, cloning, and sequence characterization of a new member of the Shc family that we termed RaLP. RaLP encodes a 69-kDa protein characterized by the CH2-PTB-CH1-SH2 modularity, typical of the Shc protein family, and expressed, among adult tissues, only in melanomas. Analysis of RaLP expression during the melanoma progression revealed low expression in normal melanocytes and benign nevi, whereas high levels of RaLP protein were found at the transition from radial growth phase to vertical growth phase and metastatic melanomas, when tumor cells acquire migratory competence and invasive potential. Notably, silencing of RaLP expression in metastatic melanomas by RNA interference reduced tumorigenesis *in vivo*. Analysis of RaLP in melanoma signal transduction pathways revealed that (a) when ectopically expressed in RaLP-negative melanocytes and nonmetastatic melanoma cells, it functions as a substrate of activated insulin-like growth factor-1 and epidermal growth factor receptors and increases Ras/mitogen-activated protein kinase (MAPK) signaling and cell migration, whereas (b) its silencing in RaLP-positive melanoma cells abrogates cell migration *in vitro*, without affecting MAPK signaling, suggesting that RaLP activates both Ras-dependent and Ras-independent migratory pathways in melanomas. These findings indicate that RaLP is a specific marker of metastatic melanomas, a critical determinant in the acquisition of the migratory phenotype by melanoma cells, and a potential target for novel anti-melanoma therapeutic strategies. [Cancer Res 2007;67(7):3064–73]

Note: Supplementary data for this article are available at Cancer Research Online (<http://cancerres.aacrjournals.org/>).

Requests for reprints: Luisa Lanfrancone, Department of Experimental Oncology, European Institute of Oncology, Via Ripamonti 435, 20141 Milan, Italy. Phone: 39-2-57489835; Fax: 39-2-57489851; E-mail: [luisa.lanfrancone@ifom-ieo-campus.it](mailto:luisa.lanfrancone@ifom-ieo-campus.it).

©2007 American Association for Cancer Research.  
doi:10.1158/0008-5472.CAN-06-2301

## Introduction

The family of Src homology and collagen (Src) genes is an example of the evolutionary success of signal transduction adaptor proteins. Its complexity increased during evolution from one locus in *Drosophila* to three loci in mammals (ShcA/Shc, ShcB/Sli, and ShcC/Rai), which encode, due to alternative initiation codon usage and splicing patterns, at least six Shc-like proteins, characterized by an NH<sub>2</sub>-terminal phosphotyrosine-binding (PTB) domain, a central region rich in proline and glycine residues (CH1) and a COOH-terminal Src homologue 2 domain (SH2) in the presented order (1). A second NH<sub>2</sub>-terminal collagen homology region (CH2) is present in the longest isoform of Shc (p66Shc; ref. 2), in p64Rai (3), and in p68Sli (4). The (CH2)-PTB-CH1-SH2 modularity is a unique feature of Shc family members (1, 5).

Despite their structural similarity, genetic and biological evidence indicate that the various Shc proteins are functionally nonredundant and regulate functions as diverse as proliferation (p52Shc), survival (p64Rai), and apoptosis and life span (p66Shc), suggesting that they are critical determinants of cell homeostasis (3, 5–8). Biochemically, they are all targets of activated tyrosine kinases (TK) but regulate different signaling events, including the activation of Ras (p52Shc), phosphatidylinositol 3-kinase (PI3K; p64Rai), and the mitochondrial permeability transition (p66Shc; refs. 3, 6, 9).

p52Shc proteins are ubiquitously expressed and are rapidly and efficiently tyrosine phosphorylated by all TKs tested thus far (5). Once phosphorylated, p52Shc facilitates recruitment of the SH2-containing growth factor receptor binding protein 2 (Grb2) adaptor protein to activated membrane receptors. The PTB and/or SH2 domains of Shc bind to tyrosine-phosphorylated receptors, whereas the SH2 of Grb2 binds to the tyrosine-phosphorylated CH1 region of Shc. Grb2, in turn, is constitutively complexed to Sos, a guanine nucleotide exchange factor of Ras. Recruitment of the Grb2/Sos complex, by p52Shc, results in the membrane relocation of Sos, an event considered sufficient to induce Ras activation. Association of phosphorylated Shc with Grb2 may also lead to the activation of Gab1, a potent activator of PI3K signaling (10).

P66Shc functions in the intracellular pathway(s) that regulates reactive oxygen species (ROS) metabolism and stress-induced apoptosis (7). A fraction of the intracellular pool of p66Shc localizes within mitochondria, where it generates ROS and regulates cytochrome *c* release (9, 11).

p64/p52Rai is expressed in the central nervous system (12–16) where it functions as a specific substrate of the RET receptor (3). Rai proteins form a constitutive complex with the p85 subunit of PI3K,

which is then recruited to ligand-activated RET receptor. Upon phosphorylation, RET stimulates neuronal cell survival by increasing PI3K activation. Notably, Rai activates PI3K also in the absence of growth factors, such as after hypoxic or oxidation insults (17).

P46Shc is a ubiquitously expressed mitochondrial protein (18); p68Sli is a cytosolic protein predominantly expressed in neurons (12, 15). Their functions remain unknown.

We report here the identification and preliminary functional characterization of a new Shc family member.

## Materials and Methods

### Cloning of RaLP

Human cDNAs containing the full-length open reading frame (ORF) was obtained by reverse transcription-PCR (RT-PCR) from total RNA of normal human and mouse skin. Oligonucleotides 1 (5'-TTTATGCAACAG-TATCCTGTTT-3') and 2 (5'-CTCAATACTGTCATTGTT-3') were used to clone the human gene; oligonucleotides 3 (5'-CTGCTAAGGCTATGCGA-GAA-3') and 4 (5'-CCGGGAGTCATCATTCTT-3') were used to clone the mouse counterpart.

### Cell Culture, Infection, and Transfection

The melanoma WM115 and WM266-4 and the fibrosarcoma HT-1080 cell lines were purchased from the American Type Culture Collection (Manassas, VA), whereas IGR-37, IGR-39, COLO-679, IGR-1, and RPMI-7951 were from Deutsche Sammlung von Mikroorganismen (Braunschweig, Germany). The melanoma COLO-853 cell line was purchased from Interlab Cell Line Collection (Genova, Italy). WM1575 were courtesy of M. Herlyn (The Wistar Institute, Philadelphia, PA). Cells were maintained as suggested by the suppliers. Normal human melanocytes were generated by dispase (Invitrogen, Carlsbad, CA) treatment of normal skin. The epidermis was disaggregated by trypsin-EDTA (Cambrex, Charles City, IA), and cells were seeded in McCoy's (Invitrogen) medium supplemented with 2% FCS, insulin (Roche, Indianapolis, IN), cholera toxin, 12-*O*-tetradecanoylphorbol-13-acetate, transferrin, hydrocortisone (Sigma-Aldrich, St. Louis, MO), stem cell factor, and fibroblast growth factor (Peprotech, Rocky Hill, NJ) and grown for several weeks.<sup>5</sup> Transfection of the Phoenix packaging cell line and infection of target cells were done as described (19), using retroviral pBABE-based vectors carrying the human RaLP (pBABE-RaLP) and p52/p46Shc (pBABE-Shc) cDNAs. For the RNA interference assays,  $9 \times 10^4$  WM266-4 cells per well were plated, in triplicate, in six-well clusters and transfected with Oligofectamine (Invitrogen) and 200 nmol/L small interfering RNAs [siRNA-RaLP(1), 5'-CCCGGCCACUUUGCUGAGUCU-3'; siRNA-RaLP(2), 5'-UCAUUGAGAUACUCUGGAUUU-3'; Luciferase, 5'-CGUACGCGGAAUACUUCGA-3' or green fluorescent protein (GFP), 5'-GGTACTCGTCCAGGAGCGCA-3'].

### Cell Proliferation and Migration Assays

**Proliferation assays.** RaLP-siRNA- and Luc-siRNA-transfected WM266-4 cells ( $9 \times 10^4$ ) were plated, in triplicate, in six-well clusters and cultured for 24, 48, and 72 h in medium containing 10% FCS. Cell viability was measured by trypan blue dye exclusion. Each experiment was done in triplicate, and means  $\pm$  SD are presented.

**Migration assays.** siRNA-transfected WM266-4 cells ( $5 \times 10^4$ ) were seeded into the upper chamber of modified Boyden chambers (Transwell, Corning-Costar, Cambridge, MA; 0.8- $\mu$ m filter pore diameter) at the indicated time points in 0.1% bovine serum albumin containing medium. In the bottom chamber, 10% fetal bovine serum was added to the medium, and the chambers were placed in humidified incubator for 24 h. Nonmigrating cells were removed with a flattened swab, and migrating cells on the underside of the chamber were stained with crystal violet solution. The extent of migration was determined by destaining migrated

cells with 10% acetic acid and measuring the absorbance at  $\lambda_{595 \text{ nm}}$ . Data are given as mean  $\pm$  SE.

### Immunoprecipitation, *In vitro* Binding Assays, and Western Blot Analysis

Cell cultures were serum starved for 48 h and treated with epidermal growth factor (EGF; Peprotech; 10 ng/mL) or insulin-like growth factor-1 (IGF-1; Peprotech; 100 ng/mL) for 10 min, if not otherwise specified. For immunoprecipitations, cell lysates were incubated with antibodies against RaLP, IGF-1 receptor (IGF-1R), EGF receptor (EGFR), and Shc. For *in vitro* binding assays, total protein lysates (1.5 mg) were incubated with 50  $\mu$ g of the appropriate glutathione *S*-transferase (GST) fusion protein. The GST-Raf assay was done as described (20). The following antibodies were used: anti-EGFR (Upstate Biotechnology, Lake Placid, NY); anti-IGF-1R and anti-extracellular signal-regulated kinase 1/2 (ERK1/2; Santa Cruz Biotechnology, Santa Cruz, CA); anti-vinculin (Sigma-Aldrich); anti-Grb2, anti-pTy, and anti-Ras (BD Transduction Laboratories, San Jose, CA); anti-AKT, anti-phosphorylated AKT (p-AKT; Ser<sup>473</sup>), and anti-phosphorylated mitogen-activated protein kinase (p-MAPK; Cell Signaling Technology, Danvers, MA). Anti-Shc antibodies have been previously generated in our laboratory and used as detailed (2). Anti-RaLP polyclonal antibodies were raised against the CH2, CH1, and SH2 domains cloned into the pGEX-2T (Invitrogen) plasmid and expressed in bacteria, as described (2).

### Immunofluorescence Analysis and Cell Fractionation

Immunofluorescence analysis was done as described (21). Briefly, cells were seeded on sterile coverslips, fixed in paraformaldehyde, permeabilized, stained with anti-RaLP antibody, and analyzed by epifluorescence.

**Cell fractionation.** Cell pellets were resuspended in ice-cold 5 mmol/L PIPES (pH 8), 1 mmol/L EGTA, 2 mmol/L DTT, and protease inhibitors; 0.5% NP40 is gently added, and lysates were centrifuged at 4°C to separate supernatant (cytoplasm) from pellet (nuclei). The separation of membrane and cytoplasmic fractions was done by the phase separation method using Triton X-114 (22). Briefly, cells were lysed in 1% Triton X-114, 10 mmol/L Tris and supernatant layered onto 6% sucrose buffer. After centrifugation, the cytoplasmic-containing fraction was recovered as aqueous phase, whereas the Triton X-114 phase, containing the membrane fraction, was recovered as a small gelatinous pellet underneath the sucrose cushion. Equal amounts of protein lysates (25  $\mu$ g) of each cellular fraction were loaded per lane and analyzed by SDS-PAGE.

### MAPK and AKT Activation Assays

Cells were serum starved for 24 h and treated with 100 ng/mL IGF-1 or 10 ng/mL EGF for 10, 30, and 60 min (p-MAPK immunoblot) or 30, 60, and 120 min (p-AKT immunoblot), before lysis; 15  $\mu$ g of total lysate were loaded and probed with anti-p-MAPK, ERK1/2, p-AKT, and AKT antibodies.

### Tissue Microarrays

For the large-scale screening study, three tissue microarrays (TMA1-TMA3) were specifically designed. Human specimens derived from formalin-fixed and paraffin-embedded tissue specimens of normal and malignant origin were analyzed. The samples were provided by the IEO Department of Pathology, Ospedale Maggiore (Novara), Presidio Ospedaliero (Vimercate), and Ospedale Sacco (Milano). Design and engineering of TMAs and *in situ* hybridization (ISH) were conducted as previously described (23). The TMAs contained 43 gastrointestinal carcinomas, 31 breast carcinomas, 25 lung carcinomas, 25 prostate carcinomas, 17 sarcomas, 12 lymphomas, 28 ovarian cancers, 25 metastatic melanomas, 15 larynx carcinomas, 19 glioblastomas, 8 papillary carcinomas, 15 carcinomas of the urinary tract, and 11 seminomas. The melanoma progression TMA includes specimens obtained from nevi, radially growing and vertically growing melanomas and metastasis.

Gene expression levels were assessed by ISH using S35-UTP-labeled sense and antisense riboprobes, as described (23). Gene expression levels were evaluated by counting the number of grains per cell, and cells were scored unequivocally positive when containing  $>25$  grains.

Immunohistochemical staining was done with anti-CH2 RaLP antibody (1:200 dilution) followed by detection with the DAKO EnVision Plus system, as previously described (23).

<sup>5</sup> G. Giardina, unpublished data.

**S.c. Implantation of Metastatic Melanoma Cells**

Nude athymic mice (6–8 weeks of age; HDS-athymic nude mice, Harlan, Udine, Italy) were implanted s.c. in the right flank either with 10<sup>6</sup> control GFP-siRNA or RaLP(1)-siRNA WM266-4 cells. The animals were kept under pathogen-free conditions in positive-pressure cabinets and observed thrice a week for the visual appearance of tumors at injection sites. Tumor growth was measured using calipers. Tumor diameter was calculated as the mean value between the shortest and longest diameter. Mice were sacrificed when tumor mass was reaching 10% of the mouse weight. Tumors were excised, and protein lysates were prepared according to established procedures.

**Results**

**Identification of RaLP.** TBLASTn analysis of the human and mouse genome with Shc, Rai, and Sli proteins from different

organisms led to the identification of a putative new member of the *Shc* gene family on human 15q21.1-q21.2 and mouse 2F1 chromosomes. The longest ORF of the homology-based reconstructed cDNAs predicts a protein with a CH2-PTB-CH1-SH2 modularity, typical of Shc-like proteins (Fig. 1A). Because the first evidences for the existence of this new gene were found searching with the *Fugu rubripes* Rai protein, this novel ORF was named RaLP (for Rai-like protein).

Human and mouse cDNAs containing the full-length ORFs were obtained by RT-PCR from total RNA of normal human and mouse skin, respectively (Genbank accession nos. AY464565 and AY464564). Their nucleotide sequence revealed an ORF of 630 and 626 AA, respectively, encoding for a putative protein of about 69 kDa. The alignment of human and mouse RaLP and human p66Shc, p64Rai, and p68Sli protein sequences is shown in Fig. 1B.

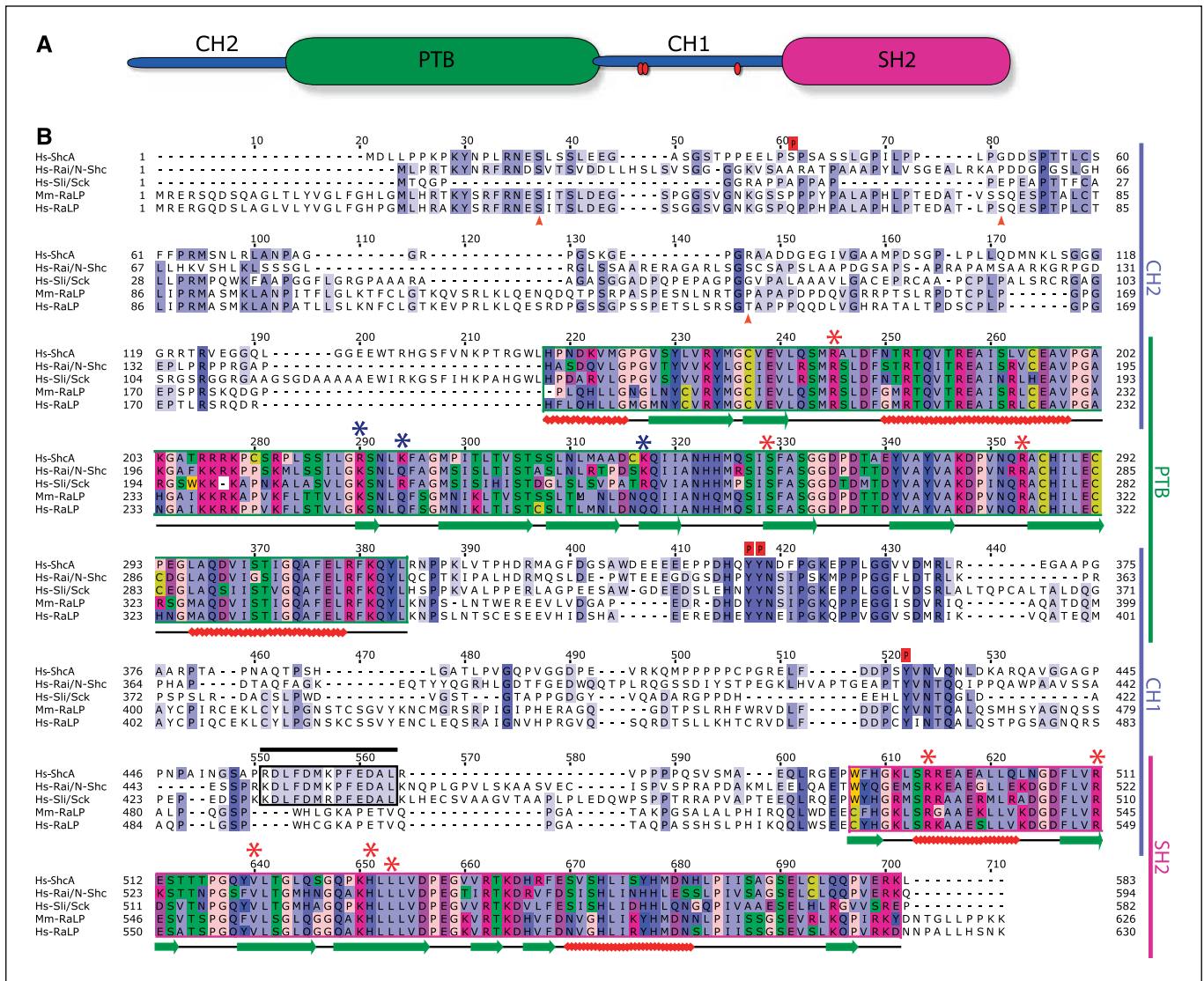


**Figure 1.** A, RaLP protein organization. The RaLP protein product is composed of two phosphotyrosine-binding domains, one located at the NH<sub>2</sub> terminus of the protein (PTB) and one at the COOH terminus (SH2). The CH1 region links the two domains; a CH2 region resides at the most NH<sub>2</sub>-terminal portion of the molecule. Tyr<sup>374/375</sup> and Tyr<sup>465</sup> are indicated by red dots in the CH1 region. B, alignment of the proteins belonging to the Shc family. Human and mouse RaLP proteins are aligned with human p66Shc, p64Rai, and p68Sli. Red asterisks, phosphotyrosine-binding pocket residues of the PTB and SH2 domains, which are strictly conserved among the four paralogues. Blue asterisks, on the contrary, charged residues directly involved in the PtdIns(4,5)P<sub>2</sub> and PtdIns(3,4,5)P<sub>3</sub> binding, which are not maintained in RaLP. Red squares, perfectly conserved CH1 tyrosine residues. Black box, points out that the amino acid stretch crucial for the interaction with the AP2 complex is entirely retained in Rai and Sli proteins but completely lost in RaLP. Red head arrows, identify S37, S76, and T142 residues as putative target residues for phosphorylation by different kinases in RaLP.



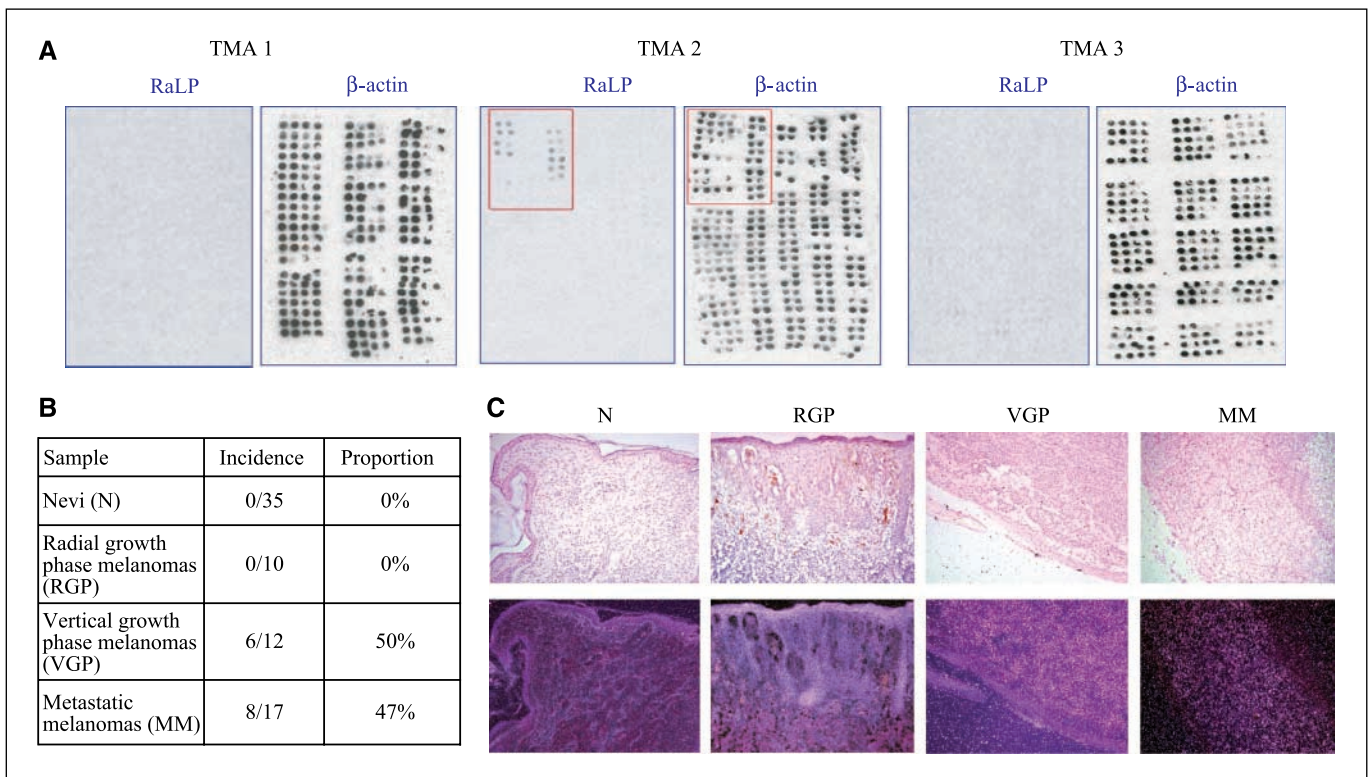


**Figure 2.** Identification of RaLP transcripts on normal and tumoral tissues. *A*, RaLP mRNA levels were analyzed by ISH on a set of TMA (TMA1, TMA2, and TMA3), which include 274 tumor specimens and 160 normal tissues. *B*, incidence of RaLP expression in a panel of melanocytic samples representing the different stages of melanoma progression. *C*, bright (*top*) and dark (*bottom*) field images of RaLP-hybridized benign nevi (N), RGP, VGP melanomas, and metastasis (MM). Positive cells are identified by the presence of silver grains.

RaLP is the most distant relative among the human Shc paralogues, with an overall identity at protein level of 37%, 41%, and 45% with Sli, Rai, and Shc, respectively (the overall identity among Shc, Sli, and Rai ranges from 44% to 47%). With respect to its modules, the RaLP PTB and SH2 domains are the most conserved (69–76% identity for the PTB region, 55–69% identity for the SH2 region, 18–24% identity for the CH1 region, and 17–25% identity for the CH2 region). The phosphotyrosine-binding pocket residues of the Shc PTB and SH2 domains, as identified by nuclear magnetic resonance, are highly conserved among the four Shc paralogues (Fig. 1*B*, *red asterisks*). The charged residues involved in the binding of the Shc PTB domain to phospholipids, which are conserved in the other members, are partially lost in RaLP (*blue asterisks*). In the CH1 region, the three tyrosine residues, which in the context of Shc and Rai are phosphorylated and bind Grb2, are conserved in RaLP, both in terms of relative position and adjacent amino acid context (*red squared "P" above the alignment*). The RDLFDMKPFE sequence of the Shc CH1 region, which is critical for its interaction with the AP2 complex, is maintained in Rai and Sli proteins but not in RaLP (*black box*). In the RaLP CH2 region, neither the S36 residue nor the EEW motif of p66Shc, which is critical for the activation of its proapoptotic function (8, 9), is conserved. These data suggest that some Shc properties (receptor and Grb2 binding) might be retained in RaLP.

**RaLP RNA expression is restricted to invasive and metastatic melanomas.** To investigate the pattern of RaLP expression in adult tissues, we analyzed levels of RaLP mRNA by ISH on a set of TMAs, which include a series of 274 of the most common tumor types and 160 normal samples. RaLP expression was detected only in

melanomas (10 of 17 cases; Fig. 2*A*). Serial sections of the same TMA hybridized with a  $\beta$ -actin probe ensured for RNA quality in the analyzed tissue samples (Fig. 2*A*). To investigate when RaLP becomes expressed during melanoma genesis and progression, we extended our analysis to a larger series of 74 pigmented lesions, including nevi (35 samples), radial growth phase (RGP; 10 samples), vertical growth phase (VGP; 12 samples), and metastatic (17 samples) melanomas. Results showed no expression of RaLP mRNA in nevi and RGP melanomas, whereas 50% of VGP and 47% of metastatic melanomas were highly positive (Fig. 2*B* and *C*). TMA data were confirmed by quantitative RT-PCR analysis, which showed low RaLP expression in nevi, intermediate in RGP melanomas, and increasingly higher in VGP and metastatic melanomas (Fig. S1*A*). It seems, therefore, that RaLP expression appears in melanomas when tumor cells acquire the ability to invade the underneath tissues.

**Identification of the RaLP protein in metastatic melanomas.** We generated anti-RaLP polyclonal antibodies in rabbits using bacterially expressed RaLP CH2 region. The resulting immune sera (*a*) specifically reacted with *in vitro* translated RaLP cDNA (data not shown), (*b*) recognized a protein of ~69 kDa in HeLa cells transiently transfected with a RaLP expression vector (Fig. 3*A*), (*c*) gave a specific immunofluorescence signal in WM266-4 melanoma cells (compared with same cells after RaLP silencing; Fig. S1*B*), and (*d*) did not cross-react with endogenous Shc proteins (Fig. S1*C*). Western blot analysis of a series of tumor cell lines showed RaLP expression only in metastatic melanomas (Fig. 3*A*, *middle*). Analysis of primary cultures of two early vertical growth melanoma samples (WM115 and IGR-39) and their metastatic counterparts (WM266-4 and IGR-37) showed higher levels in the metastatic cells (Fig. 3*A*,

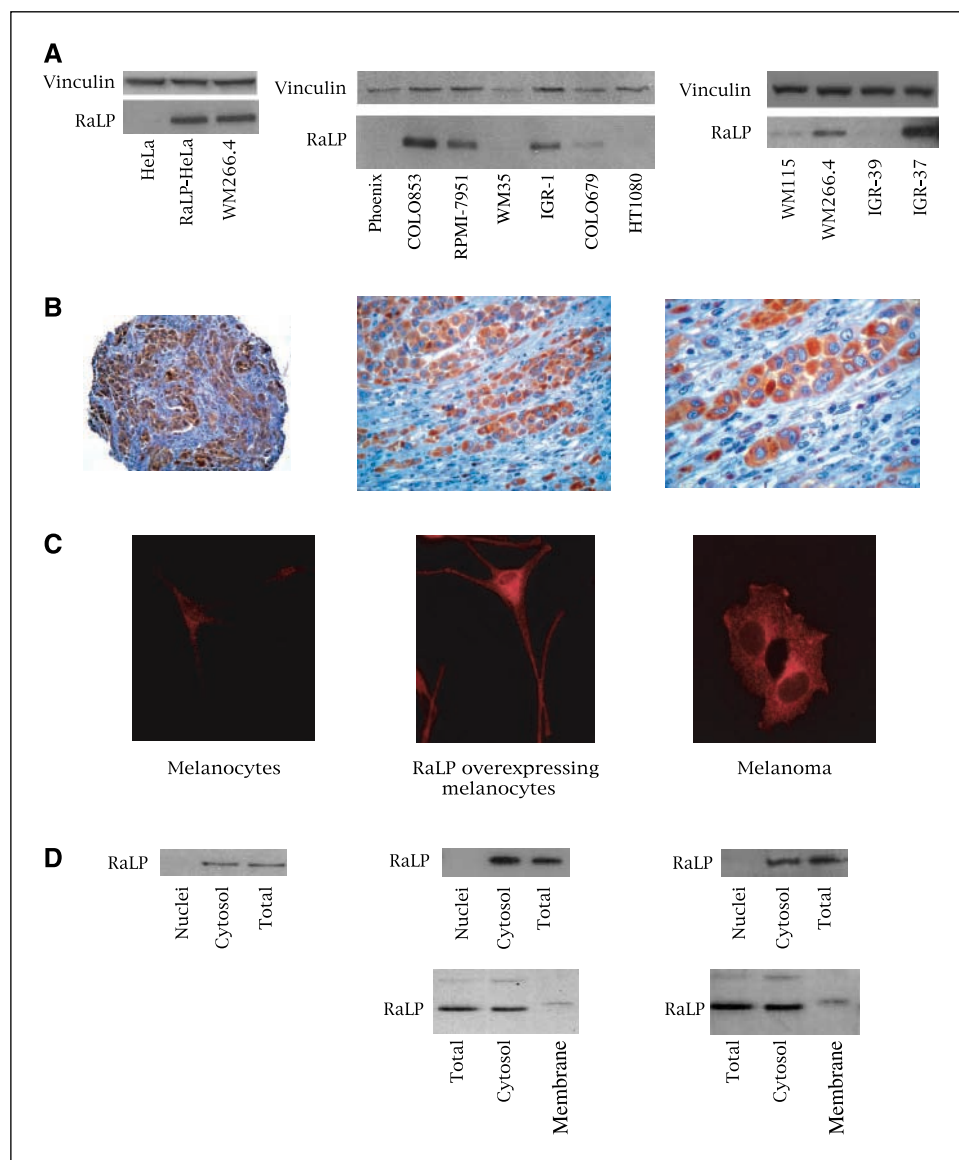


**Figure 3.** RaLP is specifically expressed in melanomas, and it is localized in the cytoplasm of the cells. *A, left*, anti-CH2 RaLP polyclonal antibody and anti-vinculin (used as loading control) staining of WM266-4 melanoma cells; HeLa and HeLa cells transiently transfected with a RaLP-expressing vector (HeLa-RaLP) served as negative and positive controls, respectively. HeLa-RaLP and WM266-4 cells express comparable levels of RaLP protein. *Middle*, RaLP protein expression in metastatic melanoma (COLO853, RPMI-7951, COLO679, WM35, and IGR-1), kidney epithelial (Phoenix), and fibrosarcoma (HT-1080) cell lines. *Right*, primary melanoma cell lines (WM115 and IGR-39) show low levels of RaLP, while the metastatic counterparts (WM266-4 and IGR-37) higher levels. *B*, RaLP immunohistochemical staining of metastatic melanoma biopsies. All neoplastic cells of the tissue reveal intense and uniform intracellular staining for RaLP protein (*brownish staining*). The blue RaLP-negative areas represent the peritumoral stroma. *C*, anti-CH2 RaLP staining on normal melanocytes, RaLP-overexpressing melanocytes, and melanoma cultures. *D*, normal melanocytes, RaLP-overexpressing melanocytes, and melanoma cells were fractionated in nuclei, cytoplasm, and membranes according to standardized protocols (see Materials and Methods). Immunoblots of fractionated lysates were probed with anti-CH2 RaLP antibody to detect the intracellular localization of the protein.

*bottom*). Immunohistochemical analysis of RaLP protein expression in paraffin-embedded samples of metastatic melanomas revealed intense and uniform intracellular staining in all tumor cells (Fig. 3B; the brownish staining corresponds to RaLP expression by tumor cells, whereas the blue areas represent the peritumoral normal stroma).

**RaLP is expressed at low levels in normal melanocytes.** We then investigated RaLP expression in normal melanocytes, by analysis of human normal skin and primary cultures of melanocytes. Quantitative RT-PCR analysis of normal skin and *in vitro* cultured melanocytes (three samples each) revealed the presence of RaLP transcripts in all samples, although at higher levels in the cultured melanocytes (Fig. S1A). ISH and immunohistochemical analysis of sections of normal skin (15 samples) revealed negativity of RaLP mRNA and protein, respectively, in all the cells of the epidermal and dermal layers (data not shown). To ensure that RaLP expression in skin melanocytes had not escaped our analysis, several normal skin biopsies were processed for RaLP ISH and immunohistochemistry and then analyzed in bright field to identify

resident brownish, melanin-containing melanocytes (data not shown). Immunofluorescence analysis of *in vitro* proliferating melanocytes showed low, yet consistently detectable, levels of RaLP protein, compared with RaLP-transduced primary melanocytes or metastatic melanomas (Fig. 3C). Together, these data suggest that RaLP expression is very low in normal resident melanocytes, and that it increases significantly when they are grown *in vitro*.

The pattern of anti-RaLP immunofluorescence staining (Fig. 3C) suggests that RaLP is a cytoplasmic protein (confirmed by nucleus-cytoplasmic fractionations; Fig. 3D). Further subcellular fractionations showed that the majority of the RaLP protein is localized in the cytosol, with only ~5% in membranes. Notably, the membrane fraction of the RaLP protein displays retarded gel migration mobility, which might be due to posttranslational modifications (Fig. 3D).

**Down-regulation of RaLP expression in melanoma cells abrogates cell migration *in vitro* and prevents tumor growth *in vivo*.** To investigate the role of RaLP in the growth and migratory phenotypes of metastatic melanomas, we

down-regulated RaLP expression by siRNAs. Transfection of RaLP-specific siRNAs into WM266-4 metastatic melanoma cells induced marked reduction of RaLP expression, compared with controls (luciferase-specific siRNAs; Fig. 4A). RaLP silencing did not affect levels of Shc proteins (Fig. S2A), did not provoke gross modifications on cell morphology (Fig. S2B), and exerted no effects on cell proliferation, as determined by cell count (Fig. 4B), cell cycle analysis, and bromodeoxyuridine incorporation (data not shown). Likewise, anti-caspase-3 staining and terminal deoxynucleotidyl transferase-mediated nick-end labeling assay did not show significant effects of RaLP silencing on apoptosis (<5% at all time points; data not shown). To investigate the role of RaLP in cell motility, RaLP-siRNA- and Luc-siRNA-transfected WM266-4 cells were seeded in a modified Boyden chamber (Transwell) in serum-free conditions and allowed to migrate towards serum. Serum-driven cell migration was almost completely inhibited in the presence of RaLP-siRNAs, compared with controls (Fig. 4C). Similar results were obtained using different RaLP-siRNA and control-siRNAs [RaLP(2)-siRNA and GFP-siRNA; Fig. 4A] and different metastatic cells (IGR-37; data not shown), thus suggesting

that continuous RaLP expression is required for *in vitro* migration of invasive melanoma cells.

We then tested if RaLP silencing blocks the tumorigenic potential of metastatic melanoma *in vivo*. Cells from the same experiment as in Fig. 4A [WM266-4 cells treated with RaLP(1)-siRNA or GFP-siRNA] were injected s.c. into nude mice. Tumor formation was monitored thrice a week for 3 weeks. RaLP down-regulation correlated with markedly reduced tumor growth (Fig. 4D). Notably, Western blotting of control and RaLP-silenced tumors taken at the end of the experiment revealed equal levels of RaLP expression (Fig. 4D), suggesting that the residual growth of the RaLP-siRNA tumors was due to emergency of rare RaLP-expressing cells. Together, these data indicate that RaLP expression is critical for the tumorigenic potential of metastatic melanoma *in vivo*.

**RaLP is a substrate of the IGF-1R and EGFR in melanoma cells.** EGF and IGF-1 play a critical role in the maintenance of growth, survival, and migration of melanoma cells *in vivo* (24–29). To investigate the role of RaLP in IGF-1 and EGF signaling, we used IGR-37 metastatic melanoma cells, which express RaLP (Fig. 3A)

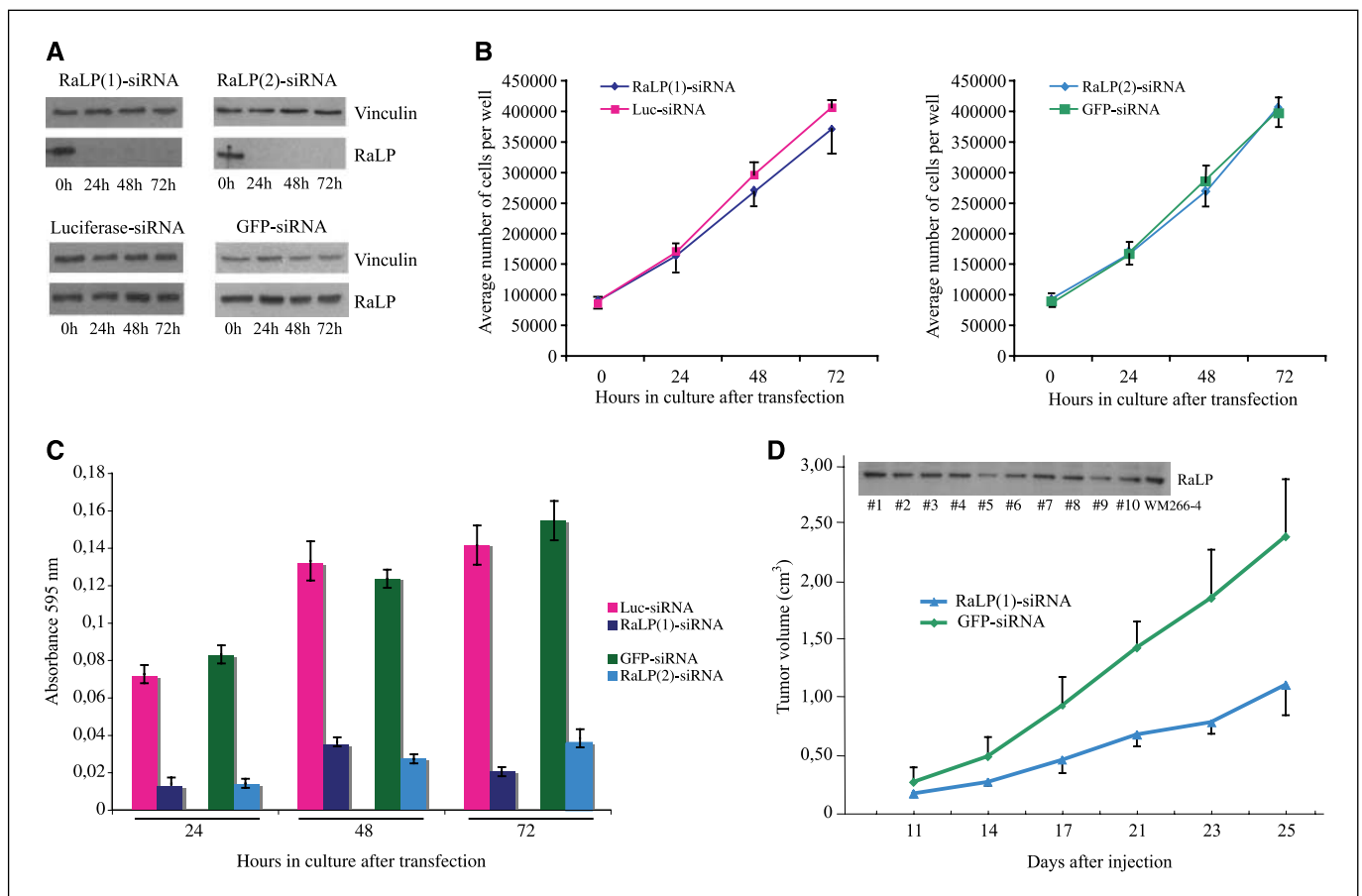


**Figure 4.** Inhibition of RaLP expression by RNA interference affects migration *in vitro* and tumorigenesis *in vivo* of melanoma cells. **A**, Western blot analysis of RaLP(1)-siRNA, RaLP(2)-siRNA, GFP-siRNA, and Luc-siRNA WM266-4 cells. Lysates were extracted at 24, 48, and 72 h upon siRNA duplex transfection and probed with anti-CH2 RaLP and anti-vinculin, as control, antibodies. **B**, proliferation assay. WM266-4 cells were plated in six-well clusters (90,000 per well) and counted in triplicate for three days after RNA interference. Points, mean from three separate determinations; bars, SD. **C**, migration assay. Cells (50,000 per well) were plated in a Transwell chamber and allowed to migrate as detailed in Materials and Methods. Extent of migration is scored by measuring the absorbance at 595 nm. Experiments were done in triplicate and repeated four times. **D**, RaLP inhibition reduces tumorigenicity of s.c. xenografted melanoma cells. Athymic *nu/nu* mice were implanted s.c. with either control GFP-siRNA or RaLP(1)-siRNA WM266-4 cells. Tumor growth is indicated as tumor volume after injection. Tumors were analyzed for RaLP expression when animals were sacrificed: tumors #1 to #5, corresponding to RaLP(1)-siRNA WM266-4 cells injected animals; tumors #6 to #10, corresponding to GFP-siRNA WM266-4 cell-injected animals. WM266-4 cell lysate is used as internal control.



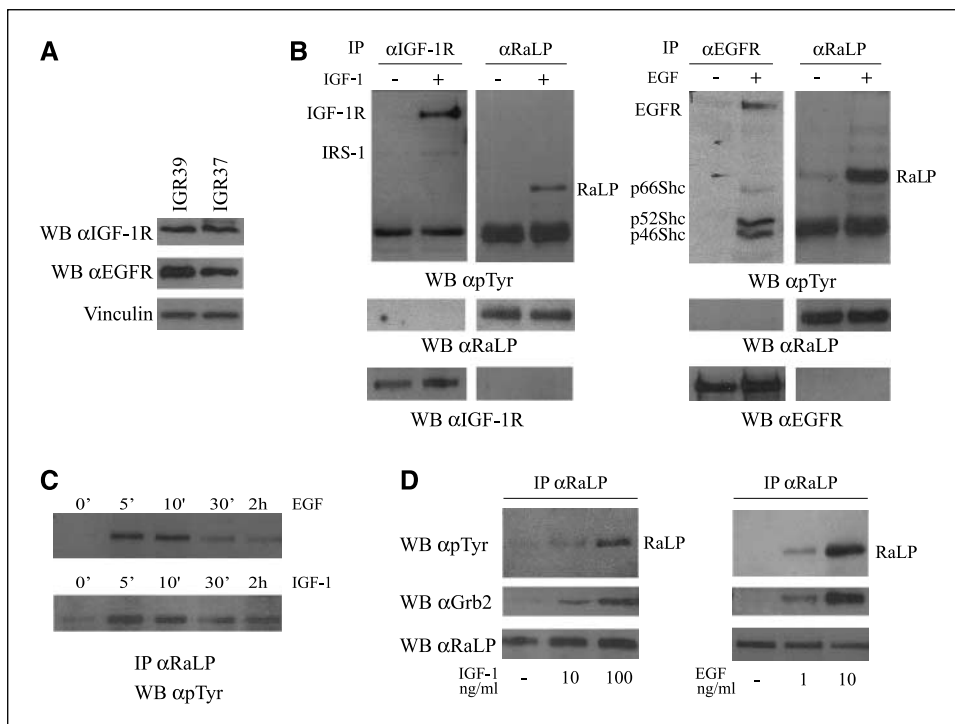


**Figure 5.** RaLP is tyrosine phosphorylated upon IGF-1 and EGF induction, and it binds to Grb2. **A**, IGF-1R and EGFR expression was evaluated in IGR-39 and IGR-37 melanoma cell lines. Vinculin was used as loading control. **WB**, Western blot. **B**, IGF-1 and EGF stimulation of IGR-37 melanoma cells induces receptors and RaLP tyrosine phosphorylation but not their physical association. Anti-RaLP, anti-IGF-1R, and anti-EGFR immunoprecipitates of IGR-37 cell lysates were analysed for anti-phosphotyrosine (pTyr), anti-RaLP, anti-IGF-1R, and anti-EGFR immunoreactivity. **C**, IGR-37 cells were treated with EGF (10 ng/mL) or IGF-1 (100 ng/mL) at the indicated time points. Anti-RaLP immunoprecipitates were probed with anti-pTyr antibody. **D**, scalar amount of EGF (1 and 10 ng/mL) and IGF-1 (10 and 100 ng/mL) induces increased RaLP phosphorylation in IGR-37. RaLP immunoprecipitates were analyzed for anti-pTyr and anti-Grb2 immunoreactivity. Anti-RaLP antibody was used as control.

and both IGF-1R and EGFR (Fig. 5A). Growth factor treatment of serum-starved IGR-37 cells induced receptor and RaLP phosphorylation (Fig. 5B). The latter occurred rapidly (5 min), was short lasting (declined after 30 min and was almost undetectable after 2 h; Fig. 5C), and depended on the amount of added IGF-1 or EGF (Fig. 5D). Notably, we did not observe additional phosphotyrosine-containing polypeptides or anti-EGFR or anti-IGF-1R immunoreactive polypeptides (Fig. 5B) in the anti-RaLP immunoprecipitates, suggesting that RaLP does not bind activated receptors (confirmed by *in vitro* pull-down experiments using GST-RaLP fusion proteins; data not shown). Blotting of anti-RaLP immunoprecipitates with anti-Grb2 antibodies revealed the existence of a ligand-inducible Grb2-RaLP complex (Fig. 5D). Pull-down experiments using GST-fusion proteins of Grb2 or Grb2-SH2 or Grb2-SH3 domains showed that the Grb2-RaLP interaction involves phosphorylated RaLP and the Grb2 SH2 domain (data not shown).

RaLP phosphorylation upon growth factor stimulation was also investigated in another metastatic melanoma cell line (WM266-4) and, upon RaLP overexpression, in primary melanocytes and the RGP WM1575, VGP WM115, and VGP IGR-39 cell lines, obtaining similar results (data not shown).

**RaLP overexpression increases IGF-1- and EGF-induced MAPK activation and migration in RGP and VGP melanoma cells.** We then investigated if RaLP increases the migratory effects of IGF-1 and EGF and if it regulates their downstream signaling pathways (PI3K or Ras). To this end, RaLP (or Shc, as positive control) was overexpressed into IGR-39 melanoma cells, which express low levels of both proteins (Fig. 6A). PI3K signaling was analyzed indirectly by measuring levels of phosphorylated AKT, a downstream target (30). No differences in AKT activation were found in control, RaLP-overexpressing, and Shc-overexpressing IGR-39 cells before or after stimulation with EGF or IGF-1 (Fig. 6D). Likewise, RaLP did not associate with IRS-1, a critical adaptor protein implicated in AKT activation by PI3K, with the p85 catalytic subunit of PI3K or with Gab1 (data not shown).

Intracellular levels of activated Ras were measured by *in vitro* binding assays using the GST-Raf fusion protein (GST-RBD), which selectively interacts with the active form of Ras (20). Anti-Ras immunoblots revealed comparable levels of total Ras protein and higher levels of activated Ras in lysates of RaLP- and Shc-overexpressing IGR-39 cells treated with EGF or IGF-1 (Fig. 6C). Accordingly, factor-stimulated RaLP- and Shc-overexpressing IGR-39 cells also showed increased levels of p-MAPK (Fig. 6D). Notably, increased levels of active Ras and p-MAPK were also detected in basal conditions (Fig. 6C and D), consistently with the finding that overexpressed Shc and RaLP proteins are moderately tyrosine phosphorylated (Fig. 6B).

Overexpression of RaLP into the IGR-39 cells (and in the RGP WM1575 cells and in primary melanocytes, which also express low levels of RaLP; see Fig. S3A) had no effects on proliferation, whereas it induced a slight (~25%), yet reproducible, increase of serum-stimulated migration (Fig. S3B; data not shown). We then tested the effects of RaLP overexpression on melanoma migration in the context of EGF and IGF-1 stimulation, using a wound-healing assay. Serum-starved WM1575 cells were scratched, induced to migrate, and scored for their capability to reconstitute the cell monolayer. RaLP-overexpressing WM1575 cells reconstituted the cell monolayer faster than control cells in response to serum, IGF-1, or EGF (Fig. S3C). Together, these data indicate that RaLP expression in melanoma cells is rate limiting for IGF-1- and EGF-induced activation of MAPK and for the ability of these growth factors (and serum) to promote cell migration. Interestingly, IGR-39 cells carry a mutated allele of B-Raf (31),<sup>6</sup> which encodes a constitutively active serine-threonine kinase, that functions upstream to Ras (32). Accordingly, MAPK is activated in melanomas with B-Raf mutations (27). The fact that Ras signaling and cell migration can

<sup>6</sup> Our unpublished data.

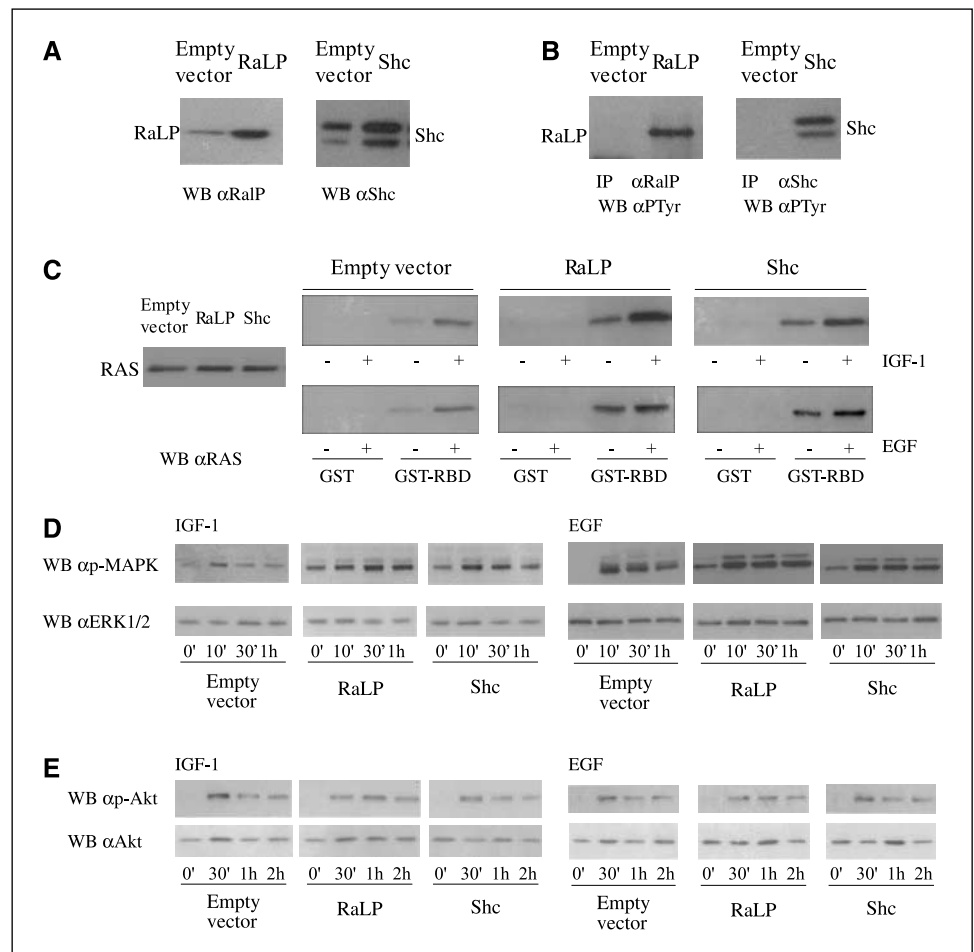
be further increased by RaLP overexpression and/or IGF-1/EGF in IGR-39 cells suggests that mutant B-Raf is not sufficient, per se, to induce maximal activation of intracellular migratory pathways in melanomas, including Ras/MAPK.

**MAPK is constitutively activated in metastatic WM266 melanoma cells and is not regulated by RaLP.** We then wished to investigate the effects of RaLP silencing on MAPK activation and migration induced by IGF-1 and EGF, using the WM266-4 metastatic melanoma cell line, which expresses high levels of endogenous RaLP and also carries a mutated B-Raf allele (33).<sup>6</sup> However, at variance with what we observed using the IGR-39 VGP melanoma cells, serum starvation or treatments with EGF or IGF-1 did not induce modifications of the levels of p-MAPK and p-AKT in WM266-4 cells (Fig. S4). Likewise, WM266-4 cells did not show any increased migratory response to EGF and IGF-1, under our experimental conditions (treatment of serum-starved cells with 0.1, 1, 10 ng/mL EGF or 1, 10, 50 ng/mL IGF-1; data not shown). Surprisingly, silencing of RaLP expression in WM266-4 metastatic cells did not modify the basal levels of MAPK (and AKT) activation either after serum starvation, or upon growth factor treatment (Fig. S4). The fact that RaLP expression is indispensable for serum-dependent migration of the same melanoma cells (Fig. 4C) suggests that RaLP might regulate additional (MAPK independent) migratory signaling pathways, which are critically activated in metastatic melanoma cells.

## Discussion

The transition from RGP melanomas, which are confined to the epidermis and yet curable, to VGP melanomas, which penetrate into the dermis and sub cutis, is critical in the evolution towards metastatic melanomas (34–40). Growth of RGP melanoma cells is tightly regulated by exogenous factors, as supplied by the surrounding keratinocytes and fibroblasts. Accordingly, RGP melanoma cells are incapable of migration and anchorage-independent growth *in vitro* and are not tumorigenic in immunodeficient mice (40). VGP melanoma cells, instead, have acquired the properties of factor/anchorage-independent growth and migration *in vitro* and develop as metastasizing tumors in experimental animal models (40). It seems, therefore, that the critical biological features of the RGP to VGP transition are the acquisition of migratory competence, growth factor independence, and invasive potential. We found high levels of RaLP expression in about half of VGP and metastatic melanomas, compared with nevi and RGP melanomas. The fact that normal melanocytes express low levels of RaLP argues against the possibility that RaLP expression in melanomas merely reflects their melanocytic origin and suggests that it is instead selected during melanoma genesis, and that it might be critical for the acquisition of the VGP and/or metastatic phenotypes. This hypothesis is supported by our finding that RaLP expression is indispensable for the growth of metastatic melanomas *in vivo*.

**Figure 6.** Tyrosine-phosphorylated RaLP induces Ras and MAPK activation but does not activate the AKT signaling pathway. **A**, IGR-39 cells were stably infected with RaLP- and Shc-containing recombinant vectors. Empty vector was used as control. RaLP and Shc protein levels were analyzed by Western blot with anti-RaLP (*left*) and anti-Shc (*right*) antibodies. **B**, total lysates of control (empty vector) and RaLP- and Shc-overexpressing IGR-39 cells were stained with anti-Ras antibody. Lysates of serum-starved RaLP- and Shc-overexpressing IGR-39 cells were immunoprecipitated with anti-RaLP (*left*) and anti-Shc (*right*) antibodies. RaLP and Shc phosphorylation was analyzed by anti-phosphotyrosine antibody and compared with cells infected with empty vector. **C**, GST pull-down assay was done with GST-RBD and GST alone in RaLP- and Shc-overexpressing IGR-39 as well as in control cells. Cells were starved for 48 h and then stimulated with 100 ng/mL IGF-1 and 10 ng/mL EGF for 10 min. **D**, IGF-1 and EGF induction stimulates MAPK phosphorylation in RaLP- and Shc-overexpressing cells. RaLP- and Shc-overexpressing IGR-39 cells are stimulated with 100 ng/mL IGF-1 and 10 ng/mL EGF at the indicated time points. MAPK phosphorylation is revealed with anti-p-MAPK antibody. Anti-ERK1/2 immunoblot served as loading control. **E**, IGF-1 and EGF stimulation does not activate the PI3K/AKT pathway. RaLP- and Shc-overexpressing IGR-39 cells were stimulated with 100 ng/mL IGF-1 and 10 ng/mL EGF at different intervals. Western blot analysis with anti-p-AKT antibody reveals that RaLP does not activate the AKT pathway. Anti-AKT immunoblot was used as loading control.





Melanocytes do not possess migratory/invasive properties, thus posing the question of where RaLP exerts its primary physiologic function. Preliminary ISH analyses of the mouse embryo (A. Simeone and LL) showed high levels of RaLP expression early during development (E7.5-E10.5), in all those territories that derive from the Neural Crest Cells (NCC) and the neural tube, and that subsequently (E12.5-16.5) originate the peripheral and the central nervous system (where RaLP is no longer expressed; ref. 41). NCCs migrate along dorsoventral and dorsolateral pathways, giving rise to neurons and glia of the peripheral nervous system, Schwann and chromaffin cells, and to founder melanoblasts, which then migrate to the skin where they differentiate into melanocytes (41). It seems, therefore, that RaLP is expressed in NCC-derived cells in the developing embryo. RaLP is also expressed in tumors of both neural crest and neural tube derivation, whereas it is not expressed in their corresponding mature cells (e.g., peripheral and central neurons). Interestingly, analysis of a large panel of nonmelanoma tumor cell lines<sup>7</sup> showed expression of RaLP only in rare cases of gliomas, neuroblastomas, and neuroectodermal tumors, which are also of neural crest and neural tube derivation. Because one relevant property of NCCs and of late-stage melanomas is their ability to migrate, re-expression of RaLP during the RGP to VGP transition might be selected by the acquired migratory phenotype.

How RaLP regulates migration in melanoma cells remains undetermined. Several growth factors and cytokines have been implicated in melanoma progression and, specifically, in the acquisition of the migratory phenotype of VGP and metastatic melanomas (24, 42). An accepted view is that the same factors that tightly control migration of normal melanocytes, nevi and RGP melanoma cells (through neighboring cells), become highly expressed in VGP and metastatic melanomas, thus imposing autocrine growth and migration potential (24). IGF-1 and EGF are among the most critical of these factors. IGF-1 is a potent stimulator for cell growth, survival, and migration of RGP and early VGP melanomas (24, 26, 27, 43, 44); it becomes highly expressed in late VGP and metastatic melanomas, which acquire autonomous proliferative and migratory properties (26, 27). Notably, attenuation

of IGF-1 signaling inhibits melanoma migration *in vitro* or melanoma growth *in vivo*, suggesting that autocrine activation of the IGF-1 signaling pathway is critical during the RGP to VGP transition (45). Likewise, EGFR signaling is required to maintain the transformed phenotype of Ras-induced melanomas *in vivo* (29).

Our data indicate that when overexpressed in RGP or VGP RaLP-negative melanoma cells, RaLP behaves as a substrate of activated IGF-1R or EGFR and stimulates migration, suggesting that it contributes to the cytoplasmic propagation of IGF-1 or EGF migratory signals in these cells. Analysis of downstream signaling pathways revealed that RaLP functions upstream to Ras. Ras/MAPK signaling, however, increases survival, growth, and migration of melanoma cells, whereas overexpression of RaLP only affects migration, suggesting that RaLP might regulate additional migratory pathways (downstream or independent to Ras). Reverse genetics experiments further supported this hypothesis. In fact, down-regulation of RaLP expression into RaLP-positive metastatic melanoma cells markedly reduced their migration potential, whereas it had no effect on the extent of MAPK activation. These findings imply that MAPK activation is not sufficient to support migration of metastatic melanomas and suggest that RaLP expression activates other critical (MAPK independent) intracellular migratory pathways. Regardless of the molecular mechanisms, which need to be further investigated, our findings indicate that RaLP is a new and apparently highly specific marker for metastatic melanoma and a biologically relevant target for the development of novel therapeutic strategies.

## Acknowledgments

Received 6/22/2006; revised 11/22/2006; accepted 1/24/2007.

**Grant support:** Ministero dell'Istruzione, dell'Università e della Ricerca FIRB project RBNE01SM99 and Associazione Italiana per la Ricerca sul Cancro Regional grant (L. Lanfrancone).

The costs of publication of this article were defrayed in part by the payment of page charges. This article must therefore be hereby marked *advertisement* in accordance with 18 U.S.C. Section 1734 solely to indicate this fact.

We thank Cristina Spinelli and Marika Zanotti for the outstanding cell culture work; Giuseppe Ossolengo for the excellent antibody preparation and purification; Ewa Aladowicz for generating the RaLP Y-F mutants; Loris Bernard and Sara Volorio for the sequencing effort; Giovanni Mazzarol, Alessandro Testori, Giulio Tosti, Massimo Mosconi, and Federica Baldini for providing and analyzing skin biopsies and melanoma samples; and Alberto Gobbi, Caterina Valetti, and Cosima Baldari for continuous support, helpful discussion, and advice.

<sup>7</sup> E. Fagiani, G. Giardina, L. Lanfrancone, unpublished data.

## References

- Luzi L, Confalonieri S, Di Fiore PP, Pelicci PG. Evolution of Shc functions from nematode to human. *Curr Opin Genet Dev* 2000;10:668-74.
- Migliaccio E, Mele S, Salcini AE, et al. Opposite effects of the p52Shc/p46Shc and p66Shc splicing isoforms on the EGF receptor-MAP kinase-*fos* signaling pathway. *EMBO J* 1997;16:706-16.
- Pelicci G, Troglio F, Bodini A, et al. The neuron-specific Rai (ShcC) adaptor protein inhibits apoptosis by coupling Ret to the phosphatidylinositol 3-kinase/Akt signaling pathway. *Mol Cell Biol* 2002;22:7351-63.
- Kojima T, Yoshikawa Y, Takada S, et al. Genomic organization of the Shc-related phosphotyrosine adaptors and characterization of the full-length Sck/ShcB: specific association of p68-Sck/ShcB with pp135. *Biochem Biophys Res Commun* 2001;284:1039-47.
- Ravichandran KS. Signaling via Shc family adapter proteins. *Oncogene* 2001;20:6322-30.
- Pelicci G, Lanfrancone L, Grignani F, et al. A novel transforming protein (SHC) with an SH2 domain is implicated in mitogenic signal transduction. *Cell* 1992;70:93-104.
- Trinei M, Giorgio M, Cicalese A, et al. A p53-66Shc signaling pathway controls intracellular redox status, levels of oxidation-damaged DNA and oxidative stress-induced apoptosis. *Oncogene* 2002;21:3872-8.
- Migliaccio E, Giorgio M, Mele S, et al. The p66shc adaptor protein controls oxidative stress response and life span in mammals. *Nature* 1999;402:309-13.
- Giorgio M, Migliaccio E, Orsini F, et al. Electron transfer between cytochrome c and p66(Shc) generates reactive oxygen species that trigger mitochondrial apoptosis. *Cell* 2005;122:221-33.
- Gu H, Neel BG. The "Gab" in signal transduction. *Trends Cell Biol* 2003;13:122-30.
- Orsini F, Migliaccio E, Moroni M, et al. The life span determinant p66Shc localizes to mitochondria where it associates with mitochondrial heat shock protein 70 and regulates trans-membrane potential. *J Biol Chem* 2004;279:25689-95.
- Nakamura T, Muraoka S, Sanokawa R, Mori N. N-Shc and Sck, two neuronally expressed Shc adapter homologs. Their differential regional expression in the brain and roles in neurotrophin and Src signaling. *J Biol Chem* 1999;273:6960-7.
- O'Bryan JP, Songyang Z, Cantley L, Der CJ, Pawson T. A mammalian adaptor protein with conserved Src homology 2 and phosphotyrosine-binding domains is related to Shc and is specifically expressed in the brain. *Proc Natl Acad Sci U S A* 1996;93:2729-34.
- Pelicci G, Dente L, De Giuseppe A, et al. A family of Shc related proteins with conserved PTB, CH1 and SH2 regions. *Oncogene* 1996;13:633-41.
- Ponti G, Conti L, Cataudella T, et al. Comparative expression profiles of ShcB and ShcC phosphotyrosine adapter molecules in the adult brain. *Neuroscience* 2005;133:105-15.
- Sakai R, Henderson JT, O'Bryan JP, Elia AJ, Saxton TM, Pawson T. The mammalian ShcB and ShcC phosphotyrosine docking proteins function in the maturation of sensory and sympathetic neurons. *Neuron* 2000;28:819-33.
- Troglio F, Echard C, Gobbi A, et al. The Rai (Shc C) adaptor protein regulates the neuronal stress response and protects against cerebral ischemia. *Proc Natl Acad Sci U S A* 2004;101:15476-81.
- Ventura A, Maccarana M, Raker VA, Pelicci PG. A cryptic targeting signal induces isoform-specific localization of p46Shc to mitochondria. *J Biol Chem* 2004;279:2299-306.

19. Grignani F, Kinsella T, Mencarelli A, et al. High-efficiency gene transfer and selection of human hematopoietic progenitor cells with a hybrid EBV/retroviral vector expressing the green fluorescence protein. *Cancer Res* 1998;58:14-9.
20. Taylor SJ, Shalloway D. Cell cycle-dependent activation of Ras. *Curr Biol* 1996;6:1621-7.
21. Lotti LV, Lanfrancone L, Migliaccio E, et al. Shc proteins are localized on endoplasmic reticulum membranes and are redistributed after tyrosine kinase receptor activation. *Mol Cell Biol* 1996;16:1946-54.
22. Plyte S, Majolini MB, Pacini S, et al. Constitutive activation of the Ras/MAP kinase pathway and enhanced TCR signaling by targeting the Shc adaptor to membrane rafts. *Oncogene* 2000;19:1529-37.
23. Nicassio F, Bianchi F, Capra M, et al. A cancer-specific transcriptional signature in human neoplasia. *J Clin Invest* 2005;115:3015-25.
24. Rodeck U, Herlyn M. Growth factors in melanoma. *Cancer Metastasis Rev* 1991;10:89-101.
25. Krasagakis K, Garbe C, Zouboulis CC, Orfanos CE. Growth control of melanoma cells and melanocytes by cytokines. *Recent Results Cancer Res* 1995;139:169-82.
26. Satyamoorthy K, Li G, Vaidya B, Kalabis J, Herlyn M. Insulin-like growth factor-I-induced migration of melanoma cells is mediated by interleukin-8 induction. *Cell Growth Differ* 2002;13:87-93.
27. Satyamoorthy K, Li G, Vaidya B, Patel D, Herlyn M. Insulin-like growth factor-1 induces survival and growth of biologically early melanoma cells through both the mitogen-activated protein kinase and beta-catenin pathways. *Cancer Res* 2001;61:7318-24.
28. Neudauer CL, McCarthy JB. Insulin-like growth factor I-stimulated melanoma cell migration requires phosphoinositide 3-kinase but not extracellular-regulated kinase activation. *Exp Cell Res* 2003;286:128-37.
29. Bardeesy N, Kim M, Xu J, et al. Role of epidermal growth factor receptor signaling in RAS-driven melanoma. *Mol Cell Biol* 2005;25:4176-88.
30. Burgering BM, Coffey PJ. Protein kinase B (c-Akt) in phosphatidylinositol-3-OH kinase signal transduction. *Nature* 1995;376:599-602.
31. Meyer P, Klaes R, Schmitt C, et al. Exclusion of BRAF<sup>V599E</sup> as a melanoma susceptibility mutation. *Int J Cancer* 2003;106:78-80.
32. Wellbrock C, Karasarides M, Marais R. The RAF proteins take centre stage. *Nat Rev Mol Cell Biol* 2004;5:875-85.
33. Davies H, Bignell GR, Cox C, et al. Mutations of the BRAF gene in human cancer. *Nature* 2002;417:949-54.
34. Reed JA, Medrano EE. Recent advances in melanoma research. *Front Biosci* 2006;11:3003-13.
35. Haass NK, Smalley KS, Li L, Herlyn M. Adhesion, migration and communication in melanocytes and melanoma. *Pigment Cell Res* 2005;18:150-9.
36. Meier F, Schitteck B, Busch S, et al. The Ras/Raf/MEK/ERK and PI3K/AKT signaling pathways present molecular targets for the effective treatment of advanced melanoma. *Front Biosci* 2005;10:2986-3001.
37. Nyormoi O, Bar-Eli M. Transcriptional regulation of metastasis-related genes in human melanoma. *Clin Exp Metastasis* 2003;20:251-63.
38. Johnson JP. Cell adhesion molecules in the development and progression of malignant melanoma. *Cancer Metastasis Rev* 1999;18:345-57.
39. Seftor RE, Seftor EA, Hendrix MJ. Molecular role(s) for integrins in human melanoma invasion. *Cancer Metastasis Rev* 1999;18:359-75.
40. Chin L. The genetics of malignant melanoma: lessons from mouse and man. *Nat Rev Cancer* 2003;3:559-70.
41. Vaglia JL, Hall BK. Regulation of neural crest cell populations: occurrence, distribution and underlying mechanisms. *Int J Dev Biol* 1999;43:95-110.
42. Lazar-Molnar E, Hegyesi H, Toth S, Falus A. Autocrine and paracrine regulation by cytokines and growth factors in melanoma. *Cytokine* 2000;12:547-54.
43. Stracke ML, Engel JD, Wilson LW, Rechler MM, Liotta LA, Schiffmann E. The type I insulin-like growth factor receptor is a motility receptor in human melanoma cells. *J Biol Chem* 1989;264:21544-9.
44. Stracke ML, Kohn EC, Aznavoorian SA, et al. Insulin-like growth factors stimulate chemotaxis in human melanoma cells. *Biochem Biophys Res Commun* 1988;153:1076-83.
45. Resnicoff M, Coppola D, Sell C, Rubin R, Ferrone S, Baserga R. Growth inhibition of human melanoma cells in nude mice by antisense strategies to the type 1 insulin-like growth factor receptor. *Cancer Res* 1994;54:4848-50.

# Cancer Research

The Journal of Cancer Research (1916–1930) | The American Journal of Cancer (1931–1940)

## RaLP, a New Member of the Src Homology and Collagen Family, Regulates Cell Migration and Tumor Growth of Metastatic Melanomas

Ernesta Fagiani, Giuseppina Giardina, Lucilla Luzi, et al.

*Cancer Res* 2007;67:3064-3073.

<b>Updated version</b>	Access the most recent version of this article at: <a href="http://cancerres.aacrjournals.org/content/67/7/3064">http://cancerres.aacrjournals.org/content/67/7/3064</a>
<b>Supplementary Material</b>	Access the most recent supplemental material at: <a href="http://cancerres.aacrjournals.org/content/suppl/2007/03/26/67.7.3064.DC1">http://cancerres.aacrjournals.org/content/suppl/2007/03/26/67.7.3064.DC1</a>

<b>Cited articles</b>	This article cites 45 articles, 13 of which you can access for free at: <a href="http://cancerres.aacrjournals.org/content/67/7/3064.full#ref-list-1">http://cancerres.aacrjournals.org/content/67/7/3064.full#ref-list-1</a>
<b>Citing articles</b>	This article has been cited by 12 HighWire-hosted articles. Access the articles at: <a href="http://cancerres.aacrjournals.org/content/67/7/3064.full#related-urls">http://cancerres.aacrjournals.org/content/67/7/3064.full#related-urls</a>

<b>E-mail alerts</b>	<a href="#">Sign up to receive free email-alerts</a> related to this article or journal.
<b>Reprints and Subscriptions</b>	To order reprints of this article or to subscribe to the journal, contact the AACR Publications Department at <a href="mailto:pubs@aacr.org">pubs@aacr.org</a> .
<b>Permissions</b>	To request permission to re-use all or part of this article, use this link <a href="http://cancerres.aacrjournals.org/content/67/7/3064">http://cancerres.aacrjournals.org/content/67/7/3064</a> . Click on "Request Permissions" which will take you to the Copyright Clearance Center's (CCC) Rightslink site.